# *Intraseasonal linkages of winter surface air temperature between Eurasia and North America*

AGU ADVANCING EARTH AND SPACE SCIENCES

Geophysical Research Letters®

RESEARCH LETTER

10.1029/2024GL113301

# Intraseasonal Linkages of Winter Surface Air Temperature Between Eurasia and North America

**Xiaocen Shen**[1], **Lin Wang**[2], **Adam A. Scaife**[3,4], **and Steven C. Hardiman**[3]

[1]Department of Meteorology, University of Reading, Reading, UK, [2]Center for Monsoon System Research, Institute of Atmospheric Physics, Chinese Academy of Sciences, Beijing, China, [3]Met Office Hadley Centre, Exeter, UK, [4]College of Engineering, Mathematics and Physical Sciences, University of Exeter, Exeter, UK

**Key Points:**

- The leading intraseasonal patterns of winter surface air temperature anomaly over Eurasia and North America (NA) show a weak but robust linkage
- Eurasia precedes an opposite-phase anomaly in NA, bridged by a tropospheric wave train and wave reflection from the stratosphere
- NA precedes a same-phase anomaly in Eurasia, mainly driven by a Scandinavian-like pattern in the troposphere

**Supporting Information:**

Supporting Information may be found in the online version of this article.

**Correspondence to:**

X. Shen,
xiaocen.shen@reading.ac.uk

**Citation:**

Shen, X., Wang, L., Scaife, A. A., & Hardiman, S. C. (2025). Intraseasonal linkages of winter surface air temperature between Eurasia and North America. *Geophysical Research Letters*, *52*, e2024GL113301. https://doi.org/10.1029/2024GL113301

Received 31 OCT 2024
Accepted 11 FEB 2025

**Author Contributions:**

**Conceptualization:** Xiaocen Shen
**Formal analysis:** Xiaocen Shen
**Investigation:** Xiaocen Shen, Lin Wang, Adam A. Scaife, Steven C. Hardiman
**Visualization:** Xiaocen Shen
**Writing – original draft:** Xiaocen Shen
**Writing – review & editing:** Lin Wang, Adam A. Scaife, Steven C. Hardiman



## Abstract

Wintertime temperature extremes sometimes show a continental linkage between Eurasia and North America (NA), but whether these connections are coincidental or dynamically robust remains unclear. This study investigates the linkages of the leading intraseasonal temperature patterns between Eurasia and NA, focusing on the underlying dynamic processes. Our findings reveal a weak but robust linkage between the dominant patterns in both regions. Specifically, an opposite-phase temperature anomaly in NA occurs about 1 week after a Eurasian temperature anomaly, influenced by wave propagation in both the troposphere and stratosphere. Conversely, a same-phase temperature anomaly appears over central Eurasia approximately 1 week after a North American temperature anomaly, primarily driven by a Scandinavian-like pattern in the troposphere. These relationships sometimes overlap, forming a sequence of temperature changes across mid-high latitudes, closely tied to the stratosphere-troposphere coupling process. The findings provide new insights for a more comprehensive understanding of wintertime intraseasonal temperature variability.

## Plain Language Summary

Both severe cold and warm extremes occur frequently in winter, especially over Eurasia and North America (NA). More importantly, winter temperature extremes sometimes occur simultaneously over the two continents. Such spatially compounded extremes can cause serious socio-economic losses, highlighting the need for a better comprehensive understanding of winter temperature variability in the midlatitudes. In this work, we found that the temperature intraseasonal variabilities over Eurasia and NA are dynamically linked, with temperature anomalies on one continent closely following the other. We further explained the reasons for this link, which involves large-scale atmospheric wave trains in both the troposphere and the stratosphere.

## 1. Introduction

In recent decades, both cold and warm extremes have been observed frequently in wintertime (e.g., Cohen et al., 2018; Gong et al., 2024; Jian et al., 2020; Wallace et al., 2014). This is most evident in Eurasia (EA) and North America (NA), where the temperature extremes exert severe impacts on society and economy (e.g., Doss-Gollin et al., 2021; Thornton et al., 2019; Yu et al., 2024). In addition, winter temperature extremes sometimes occur simultaneously in the two regions (Chen et al., 2017). For instance, cold extremes were observed in both regions in January 2006 (Si et al., 2021), reflecting an in-phase linkage. In February 2021, on the contrary, an out-of-phase temperature extreme was observed with a cold extreme in NA and a warm extreme in EA (Cohen et al., 2021; Ma & Zhu, 2023). This type of spatially compounding climate extremes can strongly amplify global and regional socio-economic impacts (Zscheischler et al., 2020), and thus requires a better understanding.

Previous studies suggest that Rossby wave trains may contribute to the intercontinental linkage of winter surface air temperature (SAT). In the midlatitudes, the zonally propagating wave trains can directly lead to large-scale circulation anomalies, facilitating the co-occurrence of extremes across continents (Lin et al., 2022; Messori & Dorrington, 2023; Xu et al., 2021). In the tropics, the Eurasian cold surge sometimes induces anomalous convection activity over the western Pacific, which then triggers a northeastward propagating wave train that affects the atmospheric circulation over the NA (Lin et al., 2022; Song et al., 2016). In addition, the Eurasian temperature anomaly can trigger and maintain the North Pacific Oscillation (Sung et al., 2021), which in turn affects North American temperature (Baxter & Nigam, 2015). Apart from tropospheric processes, variations in the stratospheric circulation can also strongly influence the large-scale tropospheric circulation over mid-high latitudes (e.g., Baldwin & Dunkerton, 2001; Ding et al., 2022; Kretschmer et al., 2018; Scaife et al., 2016), potentially leading to spatially compounded SAT anomaly across the continents.

Given the various potential pathways involved, the linkage between temperatures over the NA and EA is rather complex and can manifest on different timescales (Hou et al., 2022; Ma & Zhu, 2023). On the intraseasonal timescale, the intercontinental temperatures exhibit a lead-lag correlation (Lin, 2018), while it is unclear whether this linkage is dynamically robust, adding to the complexity of understanding the spatially compounded intercontinental SAT variations. In this work, we aim to systematically investigate the linkage of the SAT anomaly between EA and NA on the intraseasonal timescale and unravel the primary processes that contribute to the identified linkages, with the focus on both the tropospheric and stratospheric processes.

## 2. Data and Method

The daily mean reanalysis data is obtained from the fifth generation of the European Centre for Medium-Range Weather Forecasts (ERA5) data set (Hersbach et al., 2020), which extends from 1,000 to 1 hPa with 37 layers and is used at a 2.5 horizontal resolution. The period being considered spans from 1979 to 2023. The 2-m air temperature is used to represent SAT. The daily climatology is defined as the average value for each calendar day over 45 years, and the anomaly is defined as the departure from this daily climatology. The extended winter covers months from November to March (NDJFM).

As the day-to-day SAT variation in the mid-high latitudes over the Northern Hemisphere is dominated by intraseasonal components (Figure S1 in Supporting Information S1, Guan & Wang, 2023), which strongly contribute to the temperature extremes (Song et al., 2018), all subsequent analyses focus on the 10–60-day timescale. A Lanczos bandpass filter is applied to the continuous data, and the filtered NDJFM data are then extracted. The three-dimensional wave activity flux is used to diagnose the propagation of Rossby waves (Takaya & Nakamura, 2001). The two-tailed Student's $t$ test is used for the significance test.

## 3. Results

### 3.1. Lead-Lag Relationship Between the Eurasian and North American Temperature

Figures 1a and 1b show the leading modes of the daily SAT anomaly on the intraseasonal timescale identified by the empirical orthogonal function (EOF) analysis. Figure 1a is the EOF2 of the SAT variation in EA, which shows a meridional seesaw with a warming center over central Asia and a cooling center to the north. Figure 1b is the EOF1 of the SAT variation in NA, showing widespread warming in the central NA. These dominant modes are consistent with previous studies and are not sensitive if selecting slightly different regions (Guan et al., 2024; Yang & Li, 2016). It can be seen from Figure 1c that the corresponding principal component (PC) time series of the two modes have significant lead-lag correlations. When the EA pattern leads the NA pattern by 8 days, there is a negative correlation of −0.11, indicating an out-of-phase relationship between the SAT anomalies in the central EA and central NA. In contrast, when the NA pattern leads the EA pattern by 8 days, there is a positive correlation of 0.09, denoting an in-phase relationship. These two types of relationships are referred to as the EA-leading out-of-phase relationship and the NA-leading in-phase relationship, respectively. While the values are small, both are significant at 90% confidence level after considering the degree of freedom (Bretherton et al., 1999), which suggests a weak but robust relationship between the dominant temperature variability in the two regions. The EOF1 of EA has similar linkages with the NA temperature anomaly mode but is overall weaker (not shown). Given that the EOF1 and EOF2 of EA reflect a propagating oscillation (Yang & Li, 2016), it further confirms the robustness of the intercontinental linkage. In addition, the lead-lag Singular Value Decomposition approach identifies similar coupling patterns (Figure S2 in Supporting Information S1). The correlations between these two patterns were also highlighted by Lin (2018) using hemispheric-scale EOFs, further supporting the intercontinental linkages.

As the correlations are significant but weak, it is necessary to further illustrate if they are physically meaningful. To this end, the composite analysis is applied to check the evolutionary characteristics of the typical events. The temperature anomaly events are defined based on the 1.5 standard deviation ($\sigma$) threshold of the corresponding PC, with the greatest absolute value of PC occurring on day 0. The results are symmetric between cold and warm events (Figure S3 in Supporting Information S1), so we use EA warm events and NA cold events to study the EA-leading out-of-phase relationship and NA-leading in-phase relationship, respectively. Figure 1d shows the

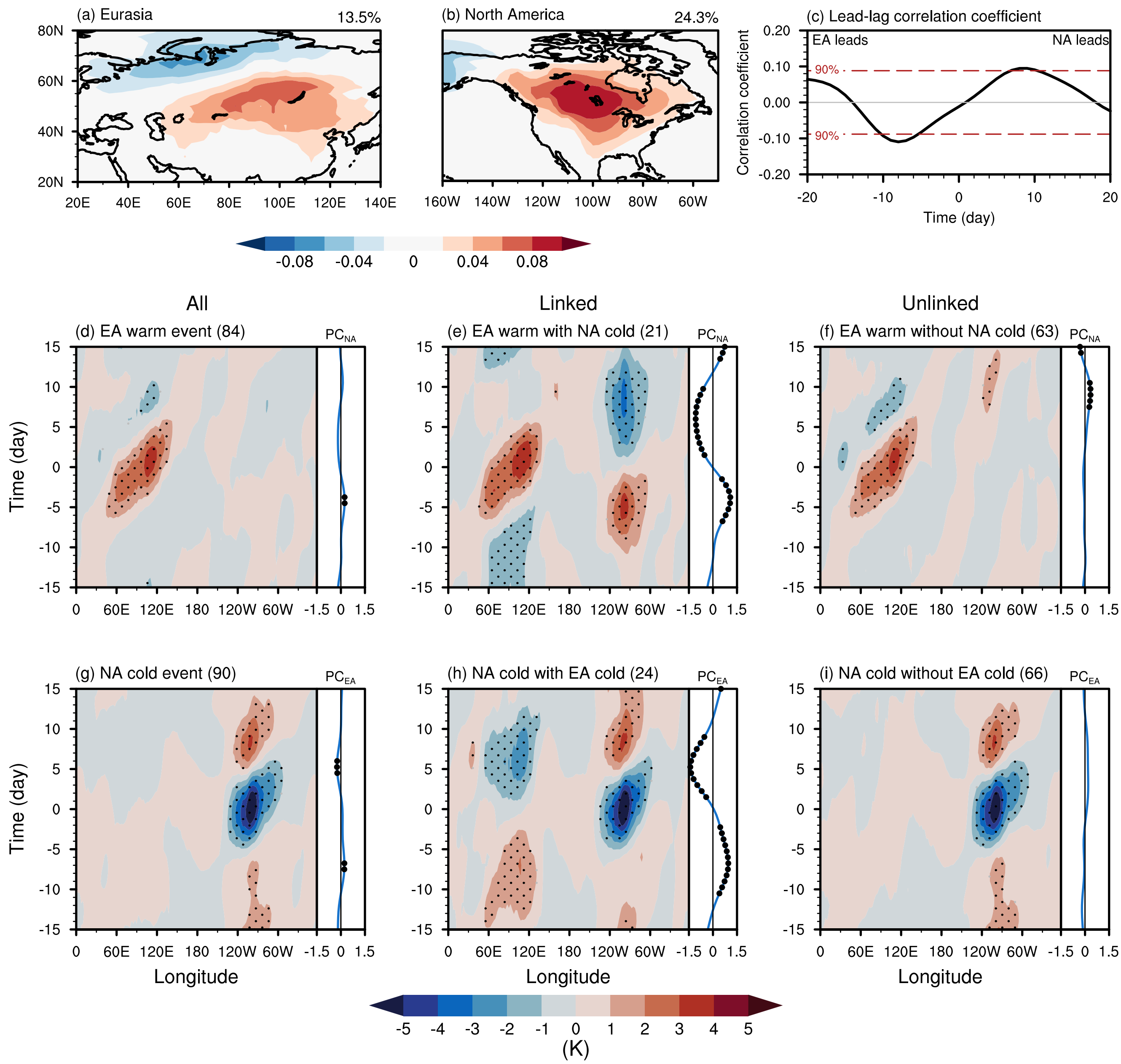


**Figure 1.** Lead-lag relationship between Eurasian and North American temperature anomalies. (a) Spatial pattern of EOF2 over the EA region (20°–140°E, 20°–80°N) based on the daily surface air temperature (SAT) anomaly in NDJFM. (b) Spatial pattern of EOF1 over the NA region (50°–160°W, 20°–80°N). The numbers on the upper right in panels (a) and (b) show the corresponding explained variance. (c) The lead-lag correlation coefficient between the principal component (PC) series corresponding to (a) and (b). The negative (positive) days mean the temperature anomaly in EA leads (lags) that in NA. The red dashed lines denote the 90% confidence level. (d)–(i) Composite longitude-time evolution of the midlatitude SAT anomaly averaged between (30°–60°N) for various types of events. The daily evolution of the PC associated with the temperature in the other continent is attached to the right side. Dots indicate values significant at the 95% confidence level. The number in the bracket shows the number of events.

longitude-time evolution of the temperature anomaly, averaged between [30°–60°N], throughout the lifecycle of EA warm events. A significant warming occurs over EA since day −7, which peaks at day 0 and gradually weakens thereafter. In the NA region, the signal is rather weak and not significant despite the overall negative value since around day −2. Similarly, for the NA cold events, there is an insignificant cold anomaly over EA following day 0 (Figure 1g).

The EA warm events are further classified according to the subsequent signal in NA. If, following day 0, the value of $PC_{NA}$ is less than $-0.75\sigma$ for at least 7 days of the 15 days, then this event is classified as a linked event. During the lifecycle of these linked events, strong and robust SAT anomalies can be seen in NA, with a significant cooling starting around day 3, peaking around day 8, and persisting until day 15 (Figure 1e), which aligns well with the statistical lagged relationship (Figure 1c). In contrast, for the unlinked events, although the EA temperature evolves similarly to the linked events, there is a slight warming over NA (Figure 1f), which may offset the out-of-phase relationship when all EA warm events are composited (Figures 1c and Figure S4 in Supporting Information S1). Similarly, for the NA cold events, the evolution of SAT over NA is nearly identical in linked and unlinked events. For the linked events, however, the SAT anomaly over EA shows a strong cooling that peaks around day 6 (Figures 1g–1i, and Figure S5 in Supporting Information S1).

With the above classification, approximately 25.00% of EA warm events are followed by strong cooling in NA, while 26.67% of NA cold events are followed by cooling in EA. Although these percentages are not very high, this is due to a strict definition aiming to capture the most strongly linked cases. Loosening the threshold value and requiring less persistence both yield more linked events. For instance, 36 linked events are identified among EA warm events if requiring the value of $PC_{NA}$ to be less than $-0.75\sigma$ for at least 5 days, increasing the proportion to 42.86%. Similarly, 39 linked events are detected for NA cold events, accounting for 43.33%. The evolution features and the associated mechanisms for the linked events are not sensitive to the thresholds (not shown), indicating the robustness of the results. As the primary goal is to investigate how these events are dynamically linked, further analysis will adhere to the strict definition to focus on the most typical, strongly linked cases.

### 3.2. Mechanism for the Eurasia Leading Out-of-Phase Relationship

Figures 2i–2l show the composite tropospheric circulation during the lifecycle of the EA warm events that are followed by cooling over NA. On day 0, a meridional dipole locates in the Eurasian region, with a low-pressure center over Northern EA and a high-pressure center over Central Asia (Figure 2j), contributing to the dipole temperature anomaly (Figure S4a in Supporting Information S1). Meanwhile, an anticyclonic anomaly intensifies around Alaska and moves westward (Figures 2j and 2k). Along with a developing cyclonic anomaly over NA (Figure 2l), this dipole structure brings cold Arctic air southward, spreading cold anomalies over large areas of NA in the following days (Figure S4a in Supporting Information S1). The development of this dipole circulation can be traced back upstream, where wave energy propagates eastward, allowing the downstream circulation to develop (vectors in Figures 2e–2l). In addition, there is a northeastward wave propagation from the Pacific (Figures 2j and 2k), underlying that the tropical circulation could also influence the temperature anomaly over NA (Guan et al., 2020; Lin et al., 2022).

One striking feature is that the circulation system is not confined within the troposphere. Instead, it shows a deep structure extending into the upper stratosphere (Figures 2a–2h). In the stratosphere, the circulation presents a westward propagating wavenumber 1 structure, with the cyclonic anomaly located over NA on day 8 (Figures 2a–2d). Associated with this, the deep circulation structure propagates westward with time, consistent with the evolution of the tropospheric circulation. In the vertical direction, the waves propagate upward and eastward from the EA then turn to propagate downward over NA (Figures 2e–2g, 2i–2k), contributing to the development of the tropospheric cyclonic anomaly over NA. This vertical wave propagation resembles the wave reflection process (e.g., Harnik & Lindzen, 2001; Perlwitz & Harnik, 2003) and has been suggested to have essential impacts on the temperature variation in NA (e.g., Kretschmer et al., 2018; Matthias & Kretschmer, 2020; Messori et al., 2022). To assess the respective role of the tropospheric and stratospheric processes in the development of the cyclonic circulation, we apply the wave activity density tendency budget (Holton, 2004; Song et al., 2016; Takaya & Nakamura, 2001). While the waves both from the stratosphere and within the troposphere play a role, the vertical component contributes more (Figure S6a in Supporting Information S1), indicating that the stratosphere-troposphere coupling is essential for causing this EA-leading out-of-phase linkage.

It is noteworthy that on day −6, the deep circulation system exhibits a structure opposite to that on day 8, consistent with the warm anomaly over NA before the occurrence of EA warming (Figure 1e and Figure S4a in Supporting Information S1). This suggests that the stratosphere-troposphere coupled system presents an oscillating feature, with the deep structure propagating clockwise over time. This behavior closely resembles the Stratosphere-Troposphere Oscillation (STO) phenomenon identified by Shen et al. (2023), the dominant stratosphere-troposphere coupling mode on the intraseasonal timescale. The wave propagation also mirrors its

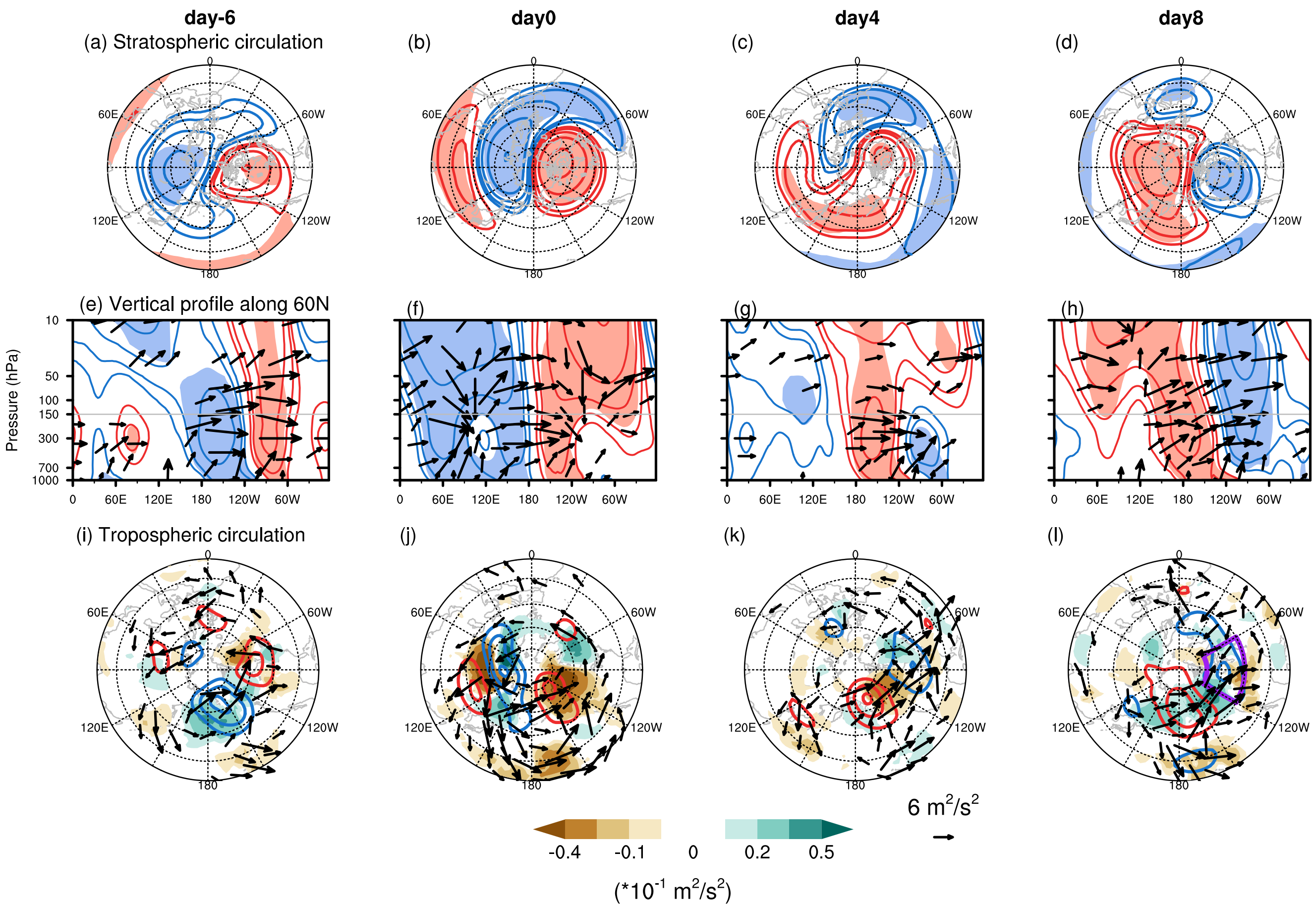


**Figure 2.** Circulation structure for the linked EA warm events. (a)–(d) Composite geopotential height anomaly at 10 hPa (Z10; contour interval is 50 gpm) on day −6, 0, 4, and 8. (e)–(h) Composite vertical profile of the geopotential height along 60°N (contour, interval is 50 gpm). (i)–(l) Composite geopotential height anomaly at 300 hPa (Z300; contour interval is 50 gpm), the associated horizontal component of wave activity flux (WAF) at 300 hPa (vector), and vertical component of WAF at 150 hPa (shading). Red and blue contours indicate positive and negative values, respectively. The zero contours are omitted. Shadings in the first and second rows indicate the region that is significant at the 95% confidence level, with the light blue and red for negative and positive values, respectively. The purple box in panel (l) is the region used to conduct the dynamic budget analysis in Figure S6 in Supporting Information S1.

counterpart throughout the lifecycle of the STO, which has been shown to drive the evolution of the deep circulation system (Shen et al., 2023). This finding indicates that the STO plays a critical role in bridging the intercontinental temperature linkage, further underscoring its importance in shaping the weather and climate across the mid-high latitudes.

### 3.3. Mechanism for the North America Leading In-Phase Relationship

The composite tropospheric circulation throughout the linked NA cold events is present in Figure 3. A northwest-southeast orientated dipole structure is seen in NA since day −5 (Figure 3a), with an anticyclonic anomaly over Bering Strait and a cyclonic anomaly over central NA. This dipole structure is similar to that in Figure 2l, confirming its role as the main contributor to the widespread SAT anomaly mode over NA (Guan et al., 2020). A wave train then propagates eastward into the Eurasian region, contributing to the rapid development of a cyclone over Scandinavia and an anticyclone around Ural Mountain (Figures 3b and 3c). The wave energy then further propagates southward, accompanied by another eastward wave propagation at lower latitudes from the North Atlantic via North Africa, contributing to the development of a cyclonic anomaly south of Lake Baikal (Figure 3c), thereby inducing the cooling over EA (Figure 1h, and Figure S5 in Supporting Information S1). The circulation then weakens (Figure 3d), consistent with the evolution of temperature over EA (Figure 1h, and Figure S5 in Supporting Information S1). This tropospheric wave structure resembles the Scandinavian pattern (Barnston & Livezey, 1987) with similar evolution characteristics on the intraseasonal timescale (Pang et al., 2021), which

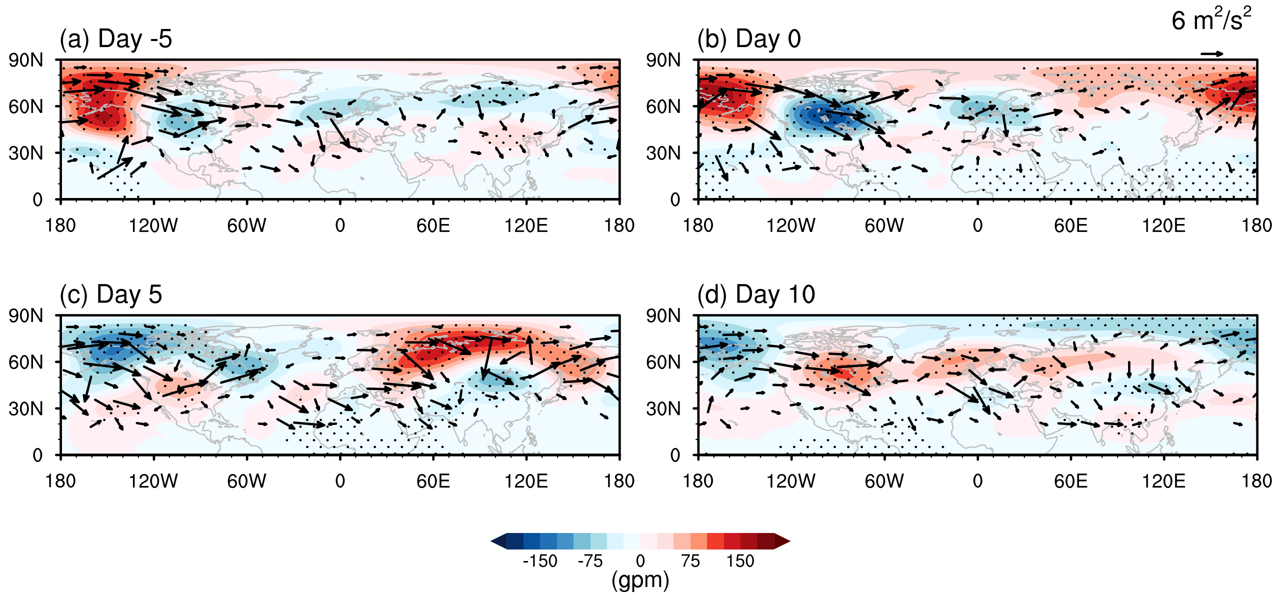


**Figure 3.** Circulation structure for the linked North America (NA) cold events. (a)–(d) The composite Z300 anomaly (shading) and associated wave activity flux at 300 hPa (vectors) on day −5, 0, 5, and 10 during the lifecycle of the linked NA cold events. The dot indicates the region where the value is significant at the 95% confidence level.

has been shown to have strong influence on the wintertime weather conditions over Eurasia (Bueh & Nakamura, 2007; Liu et al., 2014).

### 3.4. Drivers of the Different Responses in Linked and Unlinked Events

Another question is why a similar temperature anomaly is sometimes followed by a strong temperature anomaly in another continent but not at other times (Figure 1). To address this question, we systematically compare the circulation for linked and unlinked events. Figure 4a and 4b show the longitude-time evolution of the tropospheric circulation averaged between [60°–70°N] at 300 hPa (shading) for EA warm events associated with and without an NA cold anomaly. For both events, the cyclonic anomaly over Eurasia [30°–120°E] persists from day −8 to day 4 and transitions to an anticyclonic anomaly afterward. Despite the similar evolution over EA, the development of the circulation center over NA is different. In the linked events, a strong anticyclonic anomaly develops over NA (Figure 4a) and is associated with a tropospheric wave train (Figure S4a in Supporting Information S1), but these features are absent in the unlinked events (Figure 4b and Figure S4b in Supporting Information S1). In addition, the stratospheric circulation is much stronger in the linked events than in the unlinked events (contours in Figures 4a–4c). Corresponding to the strong stratospheric signal, a downward wave propagation over NA is observed around day −3 to day 5 in the linked events (red line on the right side in Figures 2j, 2k, and 4a). This wave reflection contributes to the development of the anticyclonic anomaly located around NA in the troposphere (Figure S6a in Supporting Information S1) and, thereby, the significant cold anomaly (Figure 1e and Figure S4 in Supporting Information S1). In contrast, both the tropospheric wave train and the stratospheric wave reflection are absent in the unlinked events (Figure 4b and Figure S6b in Supporting Information S1).

For the NA-leading in-phase relationship, apart from the tropospheric circulation over NA, the stratospheric circulation and vertical wave propagation are similar across linked and unlinked events (Figures 4d–4f). The most striking difference between the two types of events lies in the troposphere. In the linked events, a strong anticyclonic anomaly develops over EA around day −2 to day 12, which is not observed in the unlinked events (shading in Figures 4d–4f). This difference in tropospheric circulation is mainly related to a Scandinavian-like pattern (e.g., Bueh & Nakamura, 2007; Liu et al., 2014), which only develops in the linked events (Figure 3 and Figure S5 in Supporting Information S1). The different circulation development is not associated with the waveguide, as neither the background zonal flow nor the squared meridional wavenumber differs significantly (not shown). A closer inspection suggests that the tropospheric circulation over EA already differs from day −20

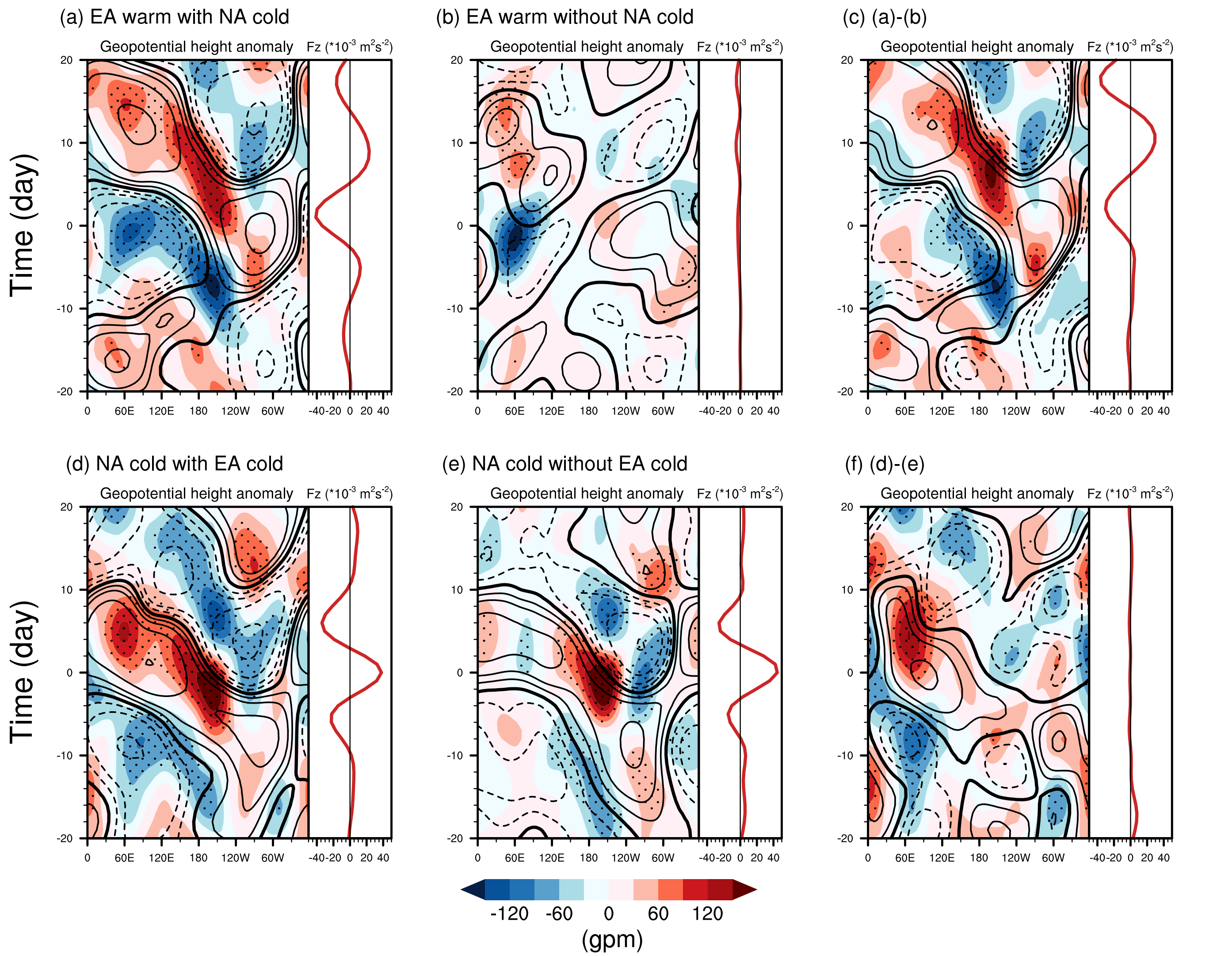


**Figure 4.** Temporal evolution of the circulation for linked and unlinked events. The longitude-time plot of the geopotential height anomalies averaged between (60°–70°N) at 300 hPa (shading; shading interval is 30 gpm) and 10 hPa (contour; contours are ±50, ±100, ±200, and ±400 gpm). The regional mean vertical wave activity flux (Fz) at 150 hPa over North America (NA) (45°–75°N, 100°–140°W) is shown on the right side. (a)–(c) The evolution of the linked and unlinked EA warm events and their differences. (d)–(f) Same as (a)–(c) but for the NA cold events. Negative contours are dashed, and zero contours are bolded. The dot indicates the region where the tropospheric anomaly is significant at the 95% confidence level.

to day −4, suggesting that the wave forcing may vary between the two types of events, but this requires further investigation.

The circulation structure and its evolution between the linked EA warm events (Figure 4a) and linked NA cold events (Figure 4d) exhibit a strong similarity. This similarity is also evident in the temperature evolution (Figures 1e and 1h and Figures S4 and S5 in Supporting Information S1), indicating possible overlaps between those two types of events, which can form a sequence of temperature changes across mid-high latitudes. It is worth mentioning that the overall circulation structure (Figure 4) and temperature response (Figures S4 and S5 in Supporting Information S1) closely resemble the evolution of the STO throughout its lifecycle (Figures 7 and 9 in Shen et al., 2023). A review of the event dates reveals a few overlapping events, most of which coincide with STO events (Table S1 in Supporting Information S1). This highlights that the STO-like stratosphere-troposphere coupling process contributes significantly to the intraseasonal swing of temperature across the two continents and thus, is essential for shaping the wintertime temperature variability over mid-high latitudes.

## 4. Summary and Discussion

In this work, we identify that the dominant winter temperature variations over the Eurasian and North American continents show dynamically robust linkages on the intraseasonal timescale. The Eurasian temperature anomaly is followed by an opposite-phase temperature anomaly over NA about 8 days later, and the North American temperature anomaly precedes a same-phase temperature anomaly in EA by 8 days. For the EA-leading out-of-phase relationship, the dipole structure over the Bering Strait and NA continent mainly plays a role, resulting from both a tropospheric wave train and stratospheric wave reflection. The NA-leading in-phase relationship is mainly induced by the Scandinavian-like pattern in the troposphere. These two linkages can occur sequentially, forming a sequence of temperature changes across mid-high latitudes, and are closely tied to the stratosphere-troposphere coupling process.

For the NA events, regardless of whether they are followed by a same-phase temperature anomaly in EA, they are always associated with a deep stratosphere-troposphere coupled system (Figures 4d and 4e). On the contrary, for the EA events, a similar stratosphere-troposphere coupling occurs only when they are followed by an opposite-phase NA anomaly (Figures 4a and 4b). This suggests that the temperature variations over NA are strongly coupled with the stratospheric variations (e.g., Ding et al., 2023; Guan et al., 2020; Hanna et al., 2024; Kidston et al., 2015; Messori et al., 2022), whereas the EA temperature anomaly is not always linked to stratospheric circulation. In future studies, it is interesting to investigate further the relative roles of stratospheric and tropospheric processes in shaping the temperature variation at mid-high latitudes.

Although these dominant temperature patterns are identified on the intraseasonal timescale, they closely resemble the long-term change pattern in the temperatures. The EA cold events resemble the warm Arctic-cold Eurasia pattern (Figure 1a; Cohen et al., 2014; Overland et al., 2011), and the cold NA events are similar to the warm Arctic-cold NA pattern (Figure 1b; Mori et al., 2014). While it is still under debate what process is primarily responsible for the warm Arctic-cold continent pattern, the results here suggest that the internal dynamics alone can generate a similar pattern on the intraseasonal timescale. Given the complex linkages between those patterns, and the paucity of monthly range prediction skill in current forecast systems (e.g., Kent et al., 2023; Vitart & Takaya, 2021), a more comprehensive understanding of the mid-high latitude intraseasonal temperature variability is needed.

## Data Availability Statement

The daily ERA5 data set is available at Hersbach et al. (2023a, 2023b).

**Acknowledgments**

We thank the two reviewers for their helpful suggestions and comments. X. S. would like to thank Xichen Li, Judah Cohen, and Marlene Kretschmer for their valuable discussions. L. W. was supported by the National Natural Science Foundation of China (41925020, 42261144687). X. S. was supported by the UK NERC Project ArctiCONNECT (NE/V005855/1) and the project XAIDA, funded through the European Union's Horizon 2020 research and innovation programme under Grant 101003469. The contributions of A. A. S. and S. C. H. were funded by the Met Office Climate Science for Service Partnership China project under the International Science Partnerships Fund.

## References

Baldwin, M. P., & Dunkerton, T. J. (2001). Stratospheric harbingers of anomalous weather regimes. *Science*, *294*(5542), 581–584. https://doi.org/10.1126/science.1063315

Barnston, A. G., & Livezey, R. E. (1987). Classification, seasonality and persistence of low-frequency atmospheric circulation patterns. *Monthly Weather Review*, *115*(6), 1083–1126. https://doi.org/10.1175/1520-0493(1987)115<1083:Csapol>2.0.Co;2

Baxter, S., & Nigam, S. (2015). Key role of the North Pacific Oscillation-West Pacific Pattern in generating the extreme 2013/14 North American winter. *Journal of Climate*, *28*(20), 8109–8117. https://doi.org/10.1175/jcli-d-14-00726.1

Bretherton, C. S., Widmann, M., Dymnikov, V. P., Wallace, J. M., & Blade, I. (1999). The effective number of spatial degrees of freedom of a time-varying field. *Journal of Climate*, *12*(7), 1990–2009. https://doi.org/10.1175/1520-0442(1999)012<1990:TENOSD>2.0.CO;2

Bueh, C., & Nakamura, H. (2007). Scandinavian pattern and its climatic impact. *Quarterly Journal of the Royal Meteorological Society*, *133*(629), 2117–2131. https://doi.org/10.1002/qj.173

Butler, A. H., Seidel, D. J., Hardiman, S. C., Butchart, N., Birner, T., & Match, A. (2015). Defining sudden stratospheric warmings. *Bulletin of the American Meteorological Society*, *96*(11), 1913–1928. https://doi.org/10.1175/bams-d-13-00173.1

Chen, R., Huang, W., Wang, B., Yang, Z., Wright, J. S., & Ma, W. (2017). On the cooccurrence of wintertime temperature anomalies over eastern Asia and eastern North America. *Journal of Geophysical Research-Atmospheres*, *122*(13), 6844–6867. https://doi.org/10.1002/2016jd026435

Cohen, J., Agel, L., Barlow, M., Garfinkel, C. I., & White, I. (2021). Linking Arctic variability and change with extreme winter weather in the United States. *Science*, *373*(6559), 1116–1121. https://doi.org/10.1126/science.abi9167

Cohen, J., Pfeiffer, K., & Francis, J. A. (2018). Warm Arctic episodes linked with increased frequency of extreme winter weather in the United States. *Nature Communications*, *9*(1), 869. https://doi.org/10.1038/s41467-018-02992-9

Cohen, J., Screen, J. A., Furtado, J. C., Barlow, M., Whittleston, D., Coumou, D., et al. (2014). Recent Arctic amplification and extreme mid-latitude weather. *Nature Geoscience*, *7*(9), 627–637. https://doi.org/10.1038/ngeo2234

Ding, X., Chen, G., Sun, L., & Zhang, P. (2022). Distinct North American cooling signatures following the zonally symmetric and asymmetric modes of winter stratospheric variability. *Geophysical Research Letters*, *49*(6), e2021GL096076. https://doi.org/10.1029/2021GL096076

Ding, X., Chen, G., Zhang, P., Domeisen, D. I. V., & Orbe, C. (2023). Extreme stratospheric wave activity as harbingers of cold events over North America. *Communications Earth & Environment*, *4*(1), 187. https://doi.org/10.1038/s43247-023-00845-y

Doss-Gollin, J., Farnham, D. J., Lall, U., & Modi, V. (2021). How unprecedented was the February 2021 Texas cold snap? *Environmental Research Letters*, *16*(6), 064056. https://doi.org/10.1088/1748-9326/ac0278

Gong, H., Ma, K., Wang, L., & Chen, W. (2024). Attribution of the record-breaking extreme cold event over northern East Asia in December 2023. *Geophysical Research Letters*, *51*(23), e2024GL112568. https://doi.org/10.1029/2024GL112568
Guan, W., Jiang, X., Ren, X., Chen, G., Lin, P., & Lin, H. (2020). The leading intraseasonal variability mode of wintertime surface air temperature over the North American sector. *Journal of Climate*, *33*(21), 9287–9306. https://doi.org/10.1175/jcli-d-20-0096.1
Guan, W., Jiang, X., Ren, X., Semenov, V., Hu, K., & Wang, L. (2024). The temperature feedback in the intraseasonal Warm Arctic–Cold North America pattern. *Atmospheric Research*, *308*, 107532. https://doi.org/10.1016/j.atmosres.2024.107532
Guan, W., & Wang, L. (2023). Mechanism of the wintertime subseasonal surface air temperature variability over Eurasia. *Environmental Research: Climate*, *2*(2), 025006. https://doi.org/10.1088/2752-5295/accd0f
Hanna, E., Francis, J., Wang, M., Overland, J. E., Cohen, J., Luo, D., et al. (2024). Influence of high-latitude blocking and the northern stratospheric polar vortex on cold-air outbreaks under Arctic amplification of global warming. *Environmental Research: Climate*, *3*(4), 042004. https://doi.org/10.1088/2752-5295/ad93f3
Harnik, N., & Lindzen, R. S. (2001). The effect of reflecting surfaces on the vertical structure and variability of stratospheric planetary waves. *Journal of the Atmospheric Sciences*, *58*(19), 2872–2894. https://doi.org/10.1175/1520-0469(2001)058<2872:Teorso>2.0.Co;2
Hersbach, H., Bell, B., Berrisford, P., Hirahara, S., Horanyi, A., Munoz-Sabater, J., et al. (2020). The ERA5 global reanalysis. *Quarterly Journal of the Royal Meteorological Society*, *146*(730), 1999–2049. https://doi.org/10.1002/qj.3803
Hersbach, H., Comyn-Platt, E., Bell, B., Berrisford, P., Biavati, G., Horányi, A., et al. (2023a). ERA5 post-processed daily-statistics on pressure levels from 1940 to present [Dataset]. *Copernicus Climate Change Service (C3S) Climate Data Store (CDS)*. https://doi.org/10.24381/cds.4991cf48
Hersbach, H., Comyn-Platt, E., Bell, B., Berrisford, P., Biavati, G., Horányi, A., et al. (2023b). ERA5 post-processed daily-statistics on pressure levels from 1940 to present [Dataset]. *Copernicus Climate Change Service (C3S) Climate Data Store (CDS)*. https://doi.org/10.24381/cds.50314f4c
Holton, J. R. (2004). *An Introduction to dynamic meteorology*. Elsevier Academic Press.
Hou, Y., Cai, W., Holland, D. M., Cheng, X., Zhang, J., Wang, L., et al. (2022). A surface temperature dipole pattern between Eurasia and North America triggered by the Barents–Kara sea-ice retreat in boreal winter. *Environmental Research Letters*, *17*(11), 114047. https://doi.org/10.1088/1748-9326/ac9ecd
Jian, Y., Lin, X., Zhou, W., Jian, M., Leung, M. Y. T., & Cheung, P. K. Y. (2020). Analysis of record-high temperature over southeast coastal China in Winter 2018/19: The combined effect of mid-to high-latitude circulation systems and SST forcing over the North Atlantic and tropical Western Pacific. *Journal of Climate*, *33*(20), 8813–8831. https://doi.org/10.1175/jcli-d-19-0732.1
Kent, C., Scaife, A. A., & Dunstone, N. (2023). What potential for improving sub-seasonal predictions of the winter NAO? *Atmospheric Science Letters*, *24*(4), e1146. https://doi.org/10.1002/asl.1146
Kidston, J., Scaife, A. A., Hardiman, S. C., Mitchell, D. M., Butchart, N., Baldwin, M. P., & Gray, L. J. (2015). Stratospheric influence on tropospheric jet streams, storm tracks and surface weather. *Nature Geoscience*, *8*(6), 433–440. https://doi.org/10.1038/ngeo2424
Kretschmer, M., Cohen, J., Matthias, V., Runge, J., & Coumou, D. (2018). The different stratospheric influence on cold-extremes in Eurasia and North America. *npj Climate and Atmospheric Science*, *1*(1), 44. https://doi.org/10.1038/s41612-018-0054-4
Lin, H. (2018). Predicting the dominant patterns of subseasonal variability of wintertime surface air temperature in extratropical Northern Hemisphere. *Geophysical Research Letters*, *45*(9), 4381–4389. https://doi.org/10.1029/2018gl077509
Lin, H., Yu, B., & Hall, N. M. J. (2022). Origin of the Warm Arctic-Cold North American pattern on the intraseasonal time scale. *Journal of the Atmospheric Sciences*, *79*(10), 2571–2583. https://doi.org/10.1175/jas-d-22-0013.1
Liu, Y., Wang, L., Zhou, W., & Chen, W. (2014). Three Eurasian teleconnection patterns: Spatial structures, temporal variability, and associated winter climate anomalies. *Climate Dynamics*, *42*(11), 2817–2839. https://doi.org/10.1007/s00382-014-2163-z
Ma, S., & Zhu, C. (2023). Subseasonal swing of cold and warm extremes between Eurasia and North America in winter of 2020/21: Initiation and physical process. *Environmental Research Letters*, *18*(1), 014023. https://doi.org/10.1088/1748-9326/acaabf
Matthias, V., & Kretschmer, M. (2020). The influence of stratospheric wave reflection on North American cold spells. *Monthly Weather Review*, *148*(4), 1675–1690. https://doi.org/10.1175/MWR-D-19-0339.1
Messori, G., & Dorrington, J. (2023). A joint perspective on North American and Euro-Atlantic weather regimes. *Geophysical Research Letters*, *50*(21), e2023GL104696. https://doi.org/10.1029/2023gl104696
Messori, G., Kretschmer, M., Lee, S. H., & Wendt, V. (2022). Stratospheric downward wave reflection events modulate North American weather regimes and cold spells. *Weather Climate Dynamics*, *3*(4), 1215–1236. https://doi.org/10.5194/wcd-3-1215-2022
Mori, M., Watanabe, M., Shiogama, H., Inoue, J., & Kimoto, M. (2014). Robust Arctic sea-ice influence on the frequent Eurasian cold winters in past decades. *Nature Geoscience*, *7*(12), 869–873. https://doi.org/10.1038/ngeo2277
Overland, J. E., Wood, K. R., & Wang, M. (2011). Warm Arctic-cold continents: Climate impacts of the newly open Arctic Sea. *Polar Research*, *30*(1), 15787. https://doi.org/10.3402/polar.v30i0.15787
Pang, B., Scaife, A. A., Lu, R., & Ren, R. (2021). Asymmetric impact of the Scandinavian pattern on stratospheric circulation anomalies. *Journal of Climate*, *34*(23), 9293–9303. https://doi.org/10.1175/JCLI-D-21-0331.1
Perlwitz, J., & Harnik, N. (2003). Observational evidence of a stratospheric influence on the troposphere by planetary wave reflection. *Journal of Climate*, *16*(18), 3011–3026. https://doi.org/10.1175/1520-0442(2003)016<3011:Oeoasi>2.0.Co;2
Scaife, A. A., Comer, R. E., Dunstone, N. J., Knight, J. R., Smith, D. M., MacLachlan, C., et al. (2017). Tropical rainfall, Rossby waves and regional winter climate predictions. *Quarterly Journal of the Royal Meteorological Society*, *143*(702), 1–11. https://doi.org/10.1002/qj.2910
Scaife, A. A., Karpechko, A. Y., Baldwin, M. P., Brookshaw, A., Butler, A. H., Eade, R., et al. (2016). Seasonal winter forecasts and the stratosphere. *Atmospheric Science Letters*, *17*(1), 51–56. https://doi.org/10.1002/asl.598
Shen, X., Wang, L., Scaife, A. A., Hardiman, S. C., & Xu, P. (2023). The Stratosphere-Troposphere Oscillation as the dominant intraseasonal coupling mode between the stratosphere and troposphere. *Journal of Climate*, *36*(7), 2259–2276. https://doi.org/10.1175/jcli-d-22-0238.1
Si, D., Jiang, D., Lang, X., & Fu, S. (2021). Unprecedented North American snowstorm and East Asian cold wave in January 2016: Critical role of the Arctic atmospheric circulation. *Atmospheric Science Letters*, *22*(11), e1056. https://doi.org/10.1002/asl.1056
Song, L., Wang, L., Chen, W., & Zhang, Y. (2016). Intraseasonal variation of the strength of the East Asian trough and its climatic impacts in boreal winter. *Journal of Climate*, *29*(7), 2557–2577. https://doi.org/10.1175/jcli-d-14-00834.1
Song, L., Wu, R., & Jiao, Y. (2018). Relative contributions of synoptic and intraseasonal variations to strong cold events over eastern China. *Climate Dynamics*, *50*(11–12), 4619–4634. https://doi.org/10.1007/s00382-017-3894-4
Sung, M. K., Son, S. W., Yoo, C., Hwang, J., & An, S. I. (2021). Seesawing of winter temperature extremes between East Asia and North America. *Journal of Climate*, *34*(11), 4423–4434. https://doi.org/10.1175/jcli-d-20-0789.1

Takaya, K., & Nakamura, H. (2001). A formulation of a phase-independent wave-activity flux for stationary and migratory quasigeostrophic eddies on a zonally varying basic flow. *Journal of the Atmospheric Sciences*, *58*(6), 608–627. https://doi.org/10.1175/1520-0469(2001)058<0608:Afoapi>2.0.Co;2

Thornton, H., Scaife, A. A., Hoskins, B. J., Brayshaw, D. J., Smith, D. M., Dunstone, N., et al. (2019). Skillful seasonal prediction of winter gas demand. *Environmental Research Letters*, *14*(2), 024009. https://doi.org/10.1088/1748-9326/aaf338

Vitart, F., & Takaya, Y. (2021). Lagged ensembles in sub-seasonal predictions. *Quarterly Journal of the Royal Meteorological Society*, *147*(739), 3227–3242. https://doi.org/10.1002/qj.4125

Wallace, J. M., Held, I. M., Thompson, D. W. J., Trenberth, K. E., & Walsh, J. E. (2014). Global warming and winter weather. *Science*, *343*(6172), 729–730. https://doi.org/10.1126/science.343.6172.729

Xu, P., Wang, L., Vallis, G. K., Geen, R., Screen, J. A., Wu, P., et al. (2021). Amplified waveguide teleconnections along the polar front jet favor summer temperature extremes over northern Eurasia. *Geophysical Research Letters*, *48*(13), e2021GL093735. https://doi.org/10.1029/2021GL093735

Yang, S., & Li, T. (2016). Intraseasonal variability of air temperature over the mid-high latitude Eurasia in boreal winter. *Climate Dynamics*, *47*(7–8), 2155–2175. https://doi.org/10.1007/s00382-015-2956-8

Yu, Y., Cui, Z., Chen, H., Liu, G., Shi, C., & Rao, J. (2024). Does the negative Arctic Oscillation always favor winter PM2.5 diffusion in North China? *Journal of Meteorological Research*, *38*(5), 954–968. https://doi.org/10.1007/s13351-024-4036-7

Zscheischler, J., Martius, O., Westra, S., Bevacqua, E., Raymond, C., Horton, R. M., et al. (2020). A typology of compound weather and climate events. *Nature Reviews Earth & Environment*, *1*(7), 333–347. https://doi.org/10.1038/s43017-020-0060-z